Investigating the Thrust Production of a Myliobatoid-Inspired Oscillating Wing

K. W. Moored[1, a], W. Smith, J. M. Hester, W. Chang, H. Bart-Smith[1,b]

[1]University of Virginia, 122 Engineers Way, Mechanical Engineering, Charlottesville, VA 22904, US

[a]kwm3x@virginia.edu, [b]hilary@virginia.edu

Keywords: Oscillation, Large amplitude, Flapping, Swimming, Rays, Biomimetic, Bio-Inspired.

Abstract. Myliobatidae is a family of large pelagic rays including cownose, eagle and manta rays. They are extremely efficient swimmers, can cruise at high speeds and can perform turn-on-a-dime maneuvering, making these fishes excellent inspiration for an autonomous underwater vehicle. Myliobatoids have been studied extensively from a biological perspective; however the fluid mechanisms that produce thrust for their large-amplitude oscillatory-style pectoral fin flapping are unknown. An experimental robotic flapping wing has been developed that closely matches the camber and planform shapes of myliobatoids. The wing can produce significant spanwise curvature, phase delays down the span, and oscillating frequencies of up to 1 Hz, capturing the dominant kinematic modes of flapping for myliobatoids. This paper uses dye flow visualization to qualitatively characterize the fluid mechanisms at work during steady-state oscillation. It is shown that oscillatory swimming uses fundamentally different fluid mechanisms than undulatory swimming by the generation of leading-edge vortices. Lessons are distilled from studying the fluid dynamics of myliobatoids that can be applied to the design of biomimetic underwater vehicles using morphing wing technology.

Introduction

In recent years, multi-disciplinary research in bio-robotic autonomous underwater vehicles (BAUVs) has grown [1, 2]. The fuel for this growth has been the potential advantages over conventional underwater vehicles such as high maneuverability, high control authority, efficient swimming mechanisms and reduced noise signatures to highlight a few. To reach some of these goals, more attention is being paid to pectoral fin hydrodynamics as their importance is realized in not only steady-state locomotion but also in transient maneuvers [1, 3-6]. Rays take pectoral fin locomotion to an evolutionary extreme, Fig. 1. Rays have a dorso-ventrally flattened body with enlarged pectoral fins that are seamlessly merged with their body to form a biological blended wing-body configuration. Even though among rays there is similar morphology, their locomotor strategies can be very different. Undulatory motion defined as having greater than one wave present on a fin [7] is one extreme of kinematic motion and was termed 'rajiform' by Breder [8]. The other extreme is oscillatory motion defined as having less than half of a wave present (flapping) on a fin and was coined 'mobuliform' by Webb [9].

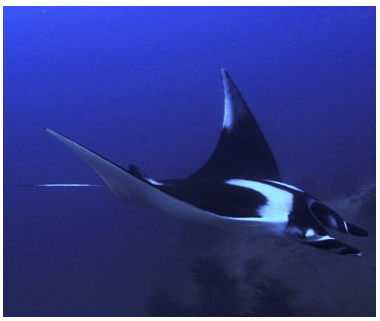

Figure 1: Image of a manta ray courtesy of www.elasmodiver.com

Although rays exhibit a continuum of kinematic motions between the two extremes [7], myliobatoids, the pelagic rays including manta, eagle, bat and cownose rays, nearly exclusively utilize oscillatory motion [10-12]. Much research has been done in the biological characteristics and behaviors of myliobatoids [13-15], but little research has been done in determining the hydrodynamics of myliobatoid's flapping motion.

Heine studied the kinematics and hydrodynamics of the cownose ray [12] by videotaping live rays swimming in a flow tank and analyzing the video. Heine used the kinematic data to attempt to determine the fluid forces acting on the rays using a quasi-static potential flow theory, but the results were not in accordance with the biological data. This negative result suggested that

unsteady mechanisms were responsible for the thrust and efficiency of rays. To qualitatively determine the mechanisms at work, Clark [16] performed flow visualization around a batoid-inspired undulating wing to construct a 3-D wake structure. They further quantified the performance of such a wing by measuring the efficiency and thrust production as well as determining an optimal gait. Their work studied low-amplitude *undulatory* (traveling wave) motion with no spanwise curvature and determined that the mechanism at work was a series of interacting trailing-edge vortices forming a reverse von Kármán street.

The scope of this paper is to extend the work of Clark [16] to study the other extreme of the batoid kinematic continuum, i.e. high-amplitude *oscillatory* (flapping) motion with significant spanwise curvature. This regime is the dominant kinematic regime for many myliobatoids [12], and its unsteady hydrodynamics have not been studied. Understanding the flow structures and the performance associated with undulatory and oscillatory swimming will greatly help future work in understanding swimming that utilizes a combination of the two, and can be applied to the design of a BAUV. Thus this paper helps give a scientific foundation for understanding oscillatory ray swimming. In particular, a robotic oscillating wing has been constructed with dye taps imbedded in its surface. Using dye flow visualization, some features of the qualitative flow structure have been determined. Finally, pertinent information is distilled from this work for application to BAUV technology.

Experiment

Setup. A robotic flapping pectoral fin has been developed to study the fluid flow structure around a myliobatoid-style fin. The robotic fin skeletal structure is a series of three hinged plates Fig. 2 cut out of Delrin in a rapid prototyping machine. The structure allows for motion only in the out-of-plane direction capturing the dominant motion of the cownose ray and other myliobatoids. Each hinge has a CK Design Technology L16-series linear actuator that controls its rotational position. Each actuator is attached to its hinge through a pulley system constructed out of aluminum 6061 machined pulleys, 0.8 mm stainless steel wire rope, copper oval crimps, and a turnbuckle. Using this pulley system gives many advantages over imbedding the actuators into the wing. First the actuators are out of the potential danger of being flooded by water and do not have to be waterproofed. Second, moving the actuators out of the fin takes unnecessary mass out of the wing and the actuators do not interfere with the final shape of the wing allowing it to have a lower profile. Lastly, the pulley system allows for the addition of a simple mechanical amplifier to maximize the force carrying capabilities and resolution of the actuators. In order to keep tension in the cables, reducing slack in the system, turnbuckles are added in-line and tightened. After tightening the turnbuckles and the tension throughout a cable route is equalized, the cables are fastened to the pulleys by set screws keeping them from slipping under the fin loading.

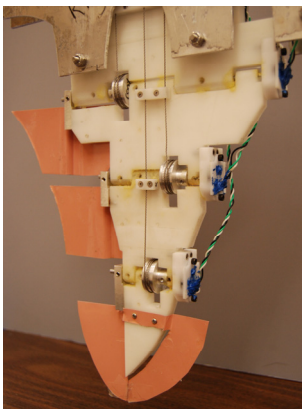

Figure 2: Internal wing structure of the robotic fin.

To measure the rotational position of each section low profile potentiometers (muRata SV01 series) were mounted to each of the aluminum shafts running through the hinges. A watertight mount was designed and created in a rapid prototyping machine for each potentiometer. The potentiometers are used as a measurement of the position of each segment giving the precise fin kinematics.

The fin skeletal structure is imbedded into a compliant PVC polymer (M-F Manufacturing, 3 parts plastic stock \#2228LP-5 and 1 part plastic softener stock \#4228S). The PVC is molded around the structure into a fin that mimics the planform shape of a cownose ray with a span length, b, of 24 cm and an average chord length, $\bar{c}$, of 18.8 cm. The cross-sectional shape varies between a NACA 0015-63 and a NACA 0029-63 from the root to the tip. The trailing edge is stiffened by sheet metal attached to the skeletal structure.

PVC tubing is imbedded in the fin on each side of the leading edge with 9, 1.6 mm ID taps spaced at approximately 2.5 cm intervals from the root to the tip. Each tube is attached to a needle valve, for flow rate variation, a solenoid valve controlled through LabVIEW, to turn on and off the dye flow, and a dye reservoir. One dye reservoir has a green dye (Sigma-Aldritch, Fluorescein sodium salt) and the other reservoir has a red dye (Aldritch, Sulforhodamine B). Both are mixed at concentrations of 50 p.p.m by weight (50 mg/L). The dye reservoirs are pressurized at 83 kPa using a compressed air reservoir and a pressure regulator.

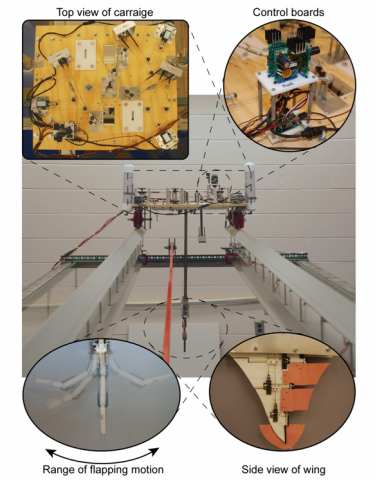

Figure 3: Carriage setup highlighting the pulley system setup, control boards, range of wing motion and wing structure.

The fin structure imbedded in PVC is fixed to a 19 mm OD aluminum tube that houses the actuating cables running to the fin and acts as a structural support which is fixed to a carriage, Fig. 3. Four stainless steel cables are attached to the tube mount at the root of the fin and are placed in tension to minimize the vibration due to the forced oscillation of the fin. The carriage acts as a platform for the pulley system, actuators, control boards, and solenoid valves. There are two acrylic windows added into the carriage platform for camera viewing. One window looks at leading-edge phenomena while the other can view the trailing-edge and wake structures. The carriage rolls along a Λ-shaped track mounted on aluminum I-beams spanning the 5 m (L) by 1.52 m (W) by 0.91 m (D) tow tank. A motor at one end of the tank pulls a v-groove belt that is attached to the carriage at speeds up to 1 m/s.

Cownose Ray Kinematic Model. To control the robotic wing a relationship between the actuator inputs and the wing section angles has been derived. The wing can be modeled as a triple pendulum system with the angles of each wing section (root, center and tip) being controlled independently through the pulley system. The angles of each section then can be simply related from input to output through a proportional gain determined by the gear ratios of the gear system, B_r, B_c and B_t.

$$\begin{aligned} \theta_r &= B_r u_r \\ \theta_c &= B_c u_c \\ \theta_t &= B_t u_t \end{aligned} \tag{1}$$

The heave is the important amplitude parameter that affects the fluid dynamics and it is the distance of the tip of the wing from its flat position. This heave is defined as

$$h = L_r \sin\theta_r + L_c \sin\theta_c + L_t \sin\theta_t . \tag{2}$$

Measured vertically, L_r is the length of the root section, L_c is the length of the center section and L_t is the length of the tip section. The actuator inputs, u_r, u_c and u_t will be restricted to vary sinusoidally all with the same frequency, f.

$$\begin{aligned} u_r &= A_r \sin\left(2\pi/f\, t + \phi_r\right) \\ u_c &= A_c \sin\left(2\pi/f\, t + \phi_c\right) \\ u_t &= A_t \sin\left(2\pi/f\, t + \phi_t\right) \end{aligned} \tag{3}$$

A_r, A_c and A_t are the amplitudes (inches of travel) of the actuators, t is the time and ϕ_r, ϕ_c and ϕ_t are the phase angles of each actuator. Combining Eq. 1, Eq. 2 and Eq. 3 and by nondimensionalizing by the average chord length of the wing, $\bar{c}$, the following relation for the heave is obtained.

$$\begin{aligned} h/\bar{c} &= L_r/\bar{c}\,\sin\left[B_r A_r \sin\left(2\pi/f\, t+\phi_r\right)\right] + L_c/\bar{c}\,\sin\left[B_c A_c \sin\left(2\pi/f\, t+\phi_c\right)\right] \\ &+ L_t/\bar{c}\,\sin\left[B_t A_t \sin\left(2\pi/f\, t+\phi_t\right)\right] \end{aligned} \tag{4}$$

In order to study different biological mechanisms, the biological kinematics need to be factored into the robot kinematics. Heine has thoroughly studied the kinematics of the cownose ray and has quantitative data of the wing curvature along the span during a flapping cycle. The curvature of the robotic wing can be matched to the data, at max deflection, giving angular relationships between the different wing sections.

$$\begin{aligned} \theta_c/\theta_r &= 3.148 \\ \theta_t/\theta_r &= 5.825 \end{aligned} \tag{5}$$

Using Eq. 5 as a set of constraints on Eq. 4 and setting the phase angles to 0, the relationship for the heave-to-chord ratio at the max deflection is defined.

$$h/\bar{c} = L_r/\bar{c}\,\sin\left(B_r A_r\right) + L_c/\bar{c}\,\sin\left(3.148 B_r A_r\right) + L_t/\bar{c}\,\sin\left(5.825 B_r A_r\right) \tag{6}$$

By limitations with the actuator travel the amplitude of the root is limited to $0 \le A_r \le 0.26$ giving a range of heave to chord ratios available for testing, $0 \le h/\bar{c} \le 0.93$.

The other fluid parameters that are important for this type of swimming are the Strouhal number, defined as $St = fh/U_\infty$ where U_∞ is the velocity of the carriage, and the Reynolds number, defined as $\mathrm{Re} = U_\infty \bar{c}/\nu$.

Results

The entire experimental setup works very well for the testing regimes that we are investigating with the dye flow visualization. In this low-speed regime the fluid forces on the wing are negligible as are the inertial forces (low velocity and acceleration). The gravitational force is also negligible since the skin-structure balances out to be neutrally buoyant. Thus the only restricting forces on the actuation are those internal to the system, e.g. friction, manufacturing errors giving rise to unmodeled forces, etc. In Fig. 4 (left) the data from the potentiometers mounted to the wing sections is shown. The dashed lines are the desired actuation profiles for each wing section and the solid lines are the actual data points taken from the potentiometers. This test was run at values of *Re = 10,000*, *St = 0.3* and $h/\bar{c} = 0.77$, which are in the regime for dye flow visualization.

This data shows the excellent quality of the actuation from the experimental setup since the actual profile is very close to the desired profile. Next, Fig. 4 (right) shows a high-speed regime ($Re = 74{,}000$, $St = 0.281$ and $h/\bar{c} = 0.73$).

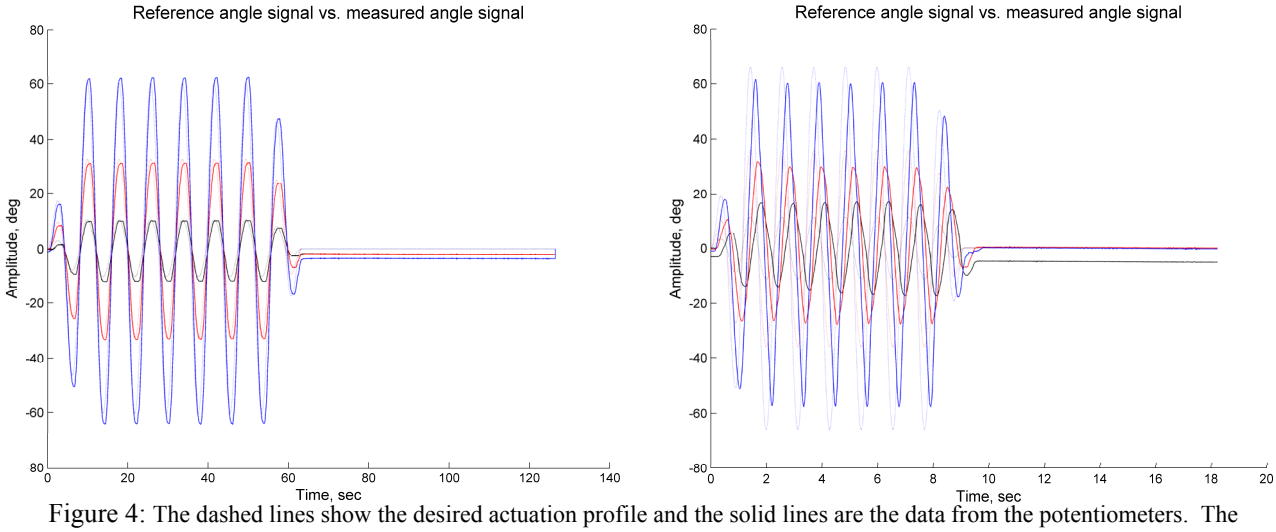

Figure 4: The dashed lines show the desired actuation profile and the solid lines are the data from the potentiometers. The blue lines are the tip section, the red lines are the center section and the black lines are the root section.

In this regime the fluid forces and inertial forces dominate and, as can be seen in the data, they have a significant effect on the actuation profile. The data shows that these forces cause the tip section to the lead the root section which is not usually an efficient mode of swimming. This suggests that if a synchronized motion is desired that the root actuator should be activated before the center and the center actuator before the tip. This can be done by making the phase angles in the kinematic model nonzero. This also suggests that in designing a BAUV wing that it is important to have phase control over segments of the wing in the span direction or the vehicles speed would be limited by inefficient swimming at high-speeds.

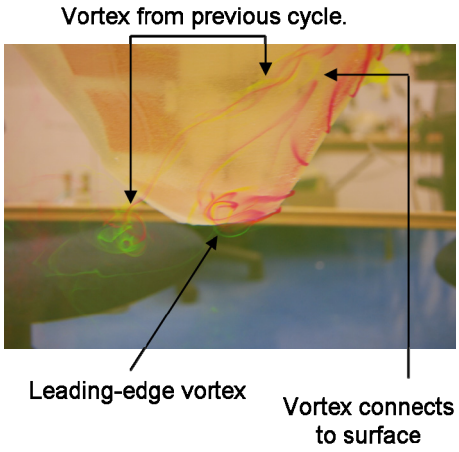

Figure 5: This image show the formation of a leading-edge vortex.

Some of the flow structures have been visualized using the dye system. In Fig. 5, a test was run at the parametric values of $Re = 548$, $St = 0.3$ and $h/\bar{c} = 0.9$. At this low of a Reynolds number the dye does not diffuse as fast and provides a clear image. Even as the Reynolds number is increased the same flow structure is seen. In this image the wing is flapping away from the camera and a leading edge vortex has formed which can be seen near the tip. The vortex is being shed across the body and is connected all the way up the surface of the water since vortices can only end on the body or at a free surface. Another vortex can also be seen from the previous cycle of flapping. The formation of a leading edge vortex was not observed in the study performed by Clark [16] investigating the undulatory mode of swimming. *Thus this new flow structure suggests that oscillatory swimming uses fundamentally different mechanisms than undulatory swimming.*

Summary and Conclusions

In this paper, an experimental setup was presented that could reproduce the oscillatory kinematic swimming mode used by many myliobatoids. It was concluded that at high-speeds a phase lead would need to be added into the root section and the center section to keep the actuation profile in synch allowing for an efficient mode of swimming. Also, it was noted that in designing a BAUV with large pectoral fins, phase control of segments along the span is necessary to be designed into wings. Lastly, it was shown that oscillatory swimming uses fundamentally different mechanisms

than undulatory motion which is important to know when studying combinations of undulation and oscillation. This also suggests that myliobatoid rays swim using leading-edge and trailing-edge vortex generation.

In future work, CFD will be used to make quantitative measurements of the flow such as thrust generated and efficiency reached. The CFD will be validated using the flow structure information that has been obtained from the dye flow visualization. After the flow structure and performance of this mode of swimming have been mapped out, new experimental setups will be developed to explore the combination between undulation and oscillation in a single wing structure. To achieve this a tensegrity morphing wing will be used.

References

[1] P. R. Bandyopadhyay, "Trends in biorobotic autonomous undersea vehicles," *IEEE Journal of Oceanic Engineering*, vol. 30, pp. 109-139, 2005.

[2] J. E. Colgate and K. M. Lynch, "Mechanics and control of swimming: a review," *Oceanic Engineering, IEEE Journal of*, vol. 29, pp. 660-673, 2004.

[3] G. V. Lauder and E. G. Drucker, "Forces, Fishes, and Fluids: Hydrodynamic Mechanisms of Aquatic Locomotion," *Physiology*, vol. 17, pp. 235-240, 2002.

[4] S. A. Combes and T. L. Daniel, "Shape, flapping and flexion: wing and fin design for forward flight," *Journal of Experimental Biology*, vol. 204, pp. 2073-2085, 2001.

[5] G. V. Lauder and E. G. Drucker, "Morphology and experimental hydrodynamics of fish fin control surfaces," *Oceanic Engineering, IEEE Journal of*, vol. 29, pp. 556-571, 2004.

[6] J. Palmisano, R. Ramamurti, K. J. Lu, J. Cohen, W. Sandberg, and B. Ratna, "Design of a Biomimetic Controlled-Curvature Robotic Pectoral Fin," *Robotics and Automation, 2007 IEEE International Conference on*, pp. 966-973, 2007.

[7] L. J. Rosenberger, "Pectoral fin locomotion in batoid fishes: undulation versus oscillation," in *Journal of Experimental Biology*, vol. 204, 2001, pp. 379-394.

[8] C. M. Breder, "The locomotion of fishes," 1926.

[9] P. W. Webb, "The biology of fish swimming," *Mechanics and Physiology of Animal Swimming*, pp. 45–62, 1994.

[10] W. Klausewitz, "Der lokomotionsmodus der Flugelrochen (Myliobatoidei)," *Zool. Anz*, vol. 173, pp. 110–120, 1964.

[11] D. E. Sasko, M. N. Dean, P. J. Motta, and R. E. Hueter, "Prey capture behavior and kinematics of the Atlantic cownose ray, Rhinoptera bonasus," *Zoology*, vol. 109, pp. 171-181, 2006.

[12] C. Heine, "Mechanics of Flapping Fin Locomotion in the Cownose Ray, Rhinoptera Bonasus (Elasmobranchii, Myliobatidae)." Duke University, 1992.

[13] J. T. Schaefer and A. P. Summers, "Batoid wing skeletal structure: Novel morphologies, mechanical implications, and phylogenetic patterns," *Journal of Morphology*, vol. 264, pp. 298-313, 2005.

[14] M. N. Dean, J. J. Bizzarro, and A. P. Summers, "The evolution of cranial design, diet, and feeding mechanisms in batoid fishes," *Integrative and Comparative Biology*, vol. 47, pp. 70, 2007.

[15] A. P. Summers, "Stiffening the stingray skeleton— an investigation of durophagy in Myliobatid stingrays(Chondrichthyes, Batoidea, Myliobatidae)," *Journal of Morphology*, vol. 243, pp. 113-126, 2000.

[16] R. P. Clark and A. J. Smits, "Thrust production and wake structure of a batoid-inspired oscillating fin," *Journal of Fluid Mechanics*, vol. 562, pp. 415-429, 2006.